RAPID COMMUNICATIONS

PHYSICAL REVIEW B VOLUME 47, NUMBER 11 15 MARCH 1993-I

Selective probing of ballistic electron orbits in rectangular antidot lattices

R. Schuster, K. Ensslin, and J. P. Kotthaus
Sektion Physik, Universität München, Geschwister-Scholl Platz 1, 8000 München 22, Germany

M. Holland and C. Stanley
Department of Electronics, University of Glasgow, Glasgow G12 8QQ, United Kingdom

(Received 3 November 1992)

Rectangular antidot lattices have been fabricated by holographic lithography and subsequent low-energy ion irradiation. The magnetoresistance depends on the direction of current flow and reveals pronounced low-field maxima that are related to ballistic electron orbits around groups of antidots. For current flow along the long period of the lattice, ballistic electron orbits around a few antidots are probed preferentially. Transport along the short period of the lattice is dominated by trajectories around many antidots. The Hall resistance is independent of the direction of current flow in agreement with symmetry arguments.

Antidot lattices represent a favorable system to study ballistic electron transport in semiconductor nanostructures. A mesh of potential pillars is imposed onto a two-dimensional electron gas to form a lateral superlattice. Transport of carriers can easily be achieved through the regions in between the antidots. In contrast, quantum-dot and quantum-wire superlattices are less accessible to transport experiments and often require high-frequency methods[1] to investigate their electronic properties. In analogy to the possible spatial anisotropy of the lattice constant of a bulk crystal various symmetries can be realized in antidot lattices. Experimentally antidot lattices with hexagonal symmetry[2] were investigated followed by studies on square lattices[3–7] and rectangular lattices.[8] Theoretically it has been shown[9,10] that the dominant features in magnetotransport experiments on square lattices are related to commensurable ballistic electron trajectories in the antidot lattice.

Here we present experimental results on rectangular antidot lattices that are fabricated by low-energy Ne-ion irradiation.[11] In this case after the fabrication process the mean free path of the carriers in the undamaged regions is almost conserved and electrons may travel ballistically along several lattice periods. Similarly as in a square lattice, electrons traverse the sample on chaotic trajectories. For certain magnetic fields pinned trajectories eventually occur that encircle an integer number of antidots. The presence of these pinned trajectories modifies the transport along the chaotic trajectories being responsible for the current transport. The magnetoresistance depends strongly on the direction of current flow with respect to the lattice orientation. A series of maxima develops for transport along the long period of the lattice while only one or two maxima occur in the perpendicular direction. Since the occurrence of pinned electron orbits around groups of antidots in the regime of linear response does not depend on any current flow, it is the conductivity of the chaotic trajectories that is responsible for the anisotropic transport behavior. From our experimental observations we conclude that small-diameter pinned orbits, which do not extend into the wide channels between the antidots, are only probed by electrons that flow through the closely spaced antidots. This idea is supported by a calculation of ballistic electron trajectories solving the classical equations of motion.

The fabrication process starts from a GaAs-$Al_xGa_{1-x}As$ heterostructure ($x=0.3$) that is grown by molecular-beam epitaxy. The structure contains a two-dimensional electron gas (2DEG) situated 60 nm below the surface. At liquid-He temperatures the carrier density is $N_s=5\times10^{11}$ cm^{-2} and the mobility $\mu=900\,000$ cm^2/V s resulting in a mean free path of the carriers of $\lambda=10$ μm. Two Hall bars that are oriented perpendicular to each other [see inset of Fig. 1(a)] are defined by wet etching. Ohmic contacts are provided by AuGe/Ni which is evaporated onto the current and voltage probes. The sample is then covered with photoresist which is exposed by an interference grating using standard holographic lithography. After a rotation of 90° around the growth axis the sample is exposed again with an interference grating of different period. Suitable exposure and development conditions lead to the removal of the photoresist in the areas of strongest exposure. A rectangular lattice of ellipsoidally shaped voids is thus formed in the photoresist. The inset of Fig. 1(b) shows an electron micrograph of a photoresist pattern that was produced this way with periods $p_x=1.0$ μm and $p_y=0.5$ μm. The detailed shape of the voids strongly depends on the anisotropy of the two in-plane periods and the development time. In the fabrication process we tried to counterbalance these two effects and keep the antidot shape as similar as possible for the various samples. For all samples discussed in this paper the short period is $p_y=0.5$ μm while the long period is varied between $p_x=0.5$ and 1.5 μm. The photoresist pattern serves as a mask for the subsequent irradiation process with low-energy Ne ions that are accelerated by a voltage of 300 V.[11] The sample resistance ρ_{xx} is monitored *in situ* during the irradiation process to allow for a reproducible resistance change of the electron gas at room temperature. The resistance ρ_{xx} for current flow along the long period p_x of the lattice is dominated by the regions between the closely spaced antidots. In order to compare the experimental results ob-

tained on samples with different $p_x:p_y$ ratios the ion dose was adjusted to result in a 30% increase of ρ_{xx} at room temperature after the low-energy irradiation process. As a final process step the sample is covered with a 5-nm-thin NiCr metal film that can be used to impose an additional electrostatic potential modulation on top of the antidot potential already created by the irradiation process.

The low-frequency (80 Hz) transport measurements are performed in a superconducting magnet ($B=0-7$ T) at liquid-He temperatures $T=4.2$ K. The magnetic field is applied perpendicular to the plane of the 2DEG. To check the importance of the numerous process parameters one sample was repeatedly both irradiated at room temperature and measured in the cryostat. Consequently all other parameters such as shape and size of the voids in the photoresist mask are identical for all measurements. The sample resistance at $B=0$ as well as the amplitude of the maxima in the low-field magnetoresistance strongly increase with increasing ion dose. However, the positions of the maxima as well as the carrier density deduced from the high-field Shubnikov–de Haas (SdH) oscillations remain independent of the ion dose in the investigated regime. We conclude that the dominant magnetoresistance features of the antidot lattice are caused by the geometric properties of the photoresist mask. The current level is varied over three orders of magnitude and Ohmic behavior is observed over the whole regime. It is therefore justified to use ideas based on the linear response theory to explain our data.

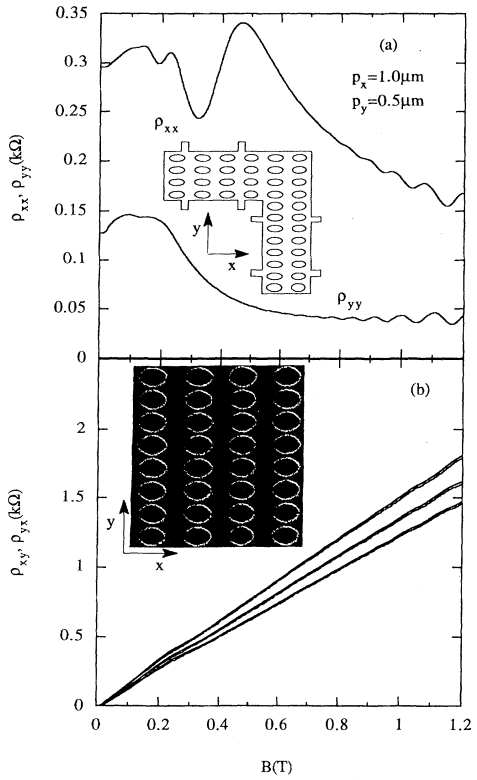

FIG. 1. (a) Magnetoresistance for current flow along the long (ρ_{xx}) and the short (ρ_{yy}) period of the lattice. The rectangular lattice has periods $p_x=1.0$ μm and $p_y=0.5$ μm. The inset presents schematically the orientation of the two Hall bars that are used in the experiment. (b) Hall resistance ρ_{xy} and ρ_{yx} for both directions of current flow for three gate voltages $V_g=0$, -400, and -800 mV. Within the accuracy of the experiment ρ_{xy} and ρ_{yx} are indistinguishable. The inset shows an electron-micrograph of the photoresist mask that was used for the irradiation process. The periods are $p_x=1.0$ μm and $p_y=0.5$ μm.

Figure 1(a) presents experimental results for the magnetoresistance ρ_{xx} along the long period ($p_x=1.0$ μm) of the lattice and ρ_{yy} along the short period ($p_y=0.5$ μm). The inset clarifies the orientation. We will first present a detailed discussion of this sample with $p_x:p_y=2:1$ $=1.0$ μm:0.5 μm and later compare samples with different ratios of the periods. At $B=0$ ρ_{xx} is larger than ρ_{yy} as expected from geometric considerations. For current flow along the long period of the lattice (ρ_{xx}) the resistance is limited by the region of the 2DEG between two closely spaced antidots. In contrast, for current flow along the short period (ρ_{yy}) the electrons traverse through the wide channels between the rows of antidots and the resistance is only moderately increased as compared to the nonirradiated sample.

Three pronounced maxima emerge in ρ_{xx} for $0<B<0.6$ T. Simultaneously only one significant feature develops in ρ_{yy} in the same range of magnetic fields [see Fig. 1(a)]. For high magnetic fields $B>0.8$ T SdH oscillations become apparent. Figure 1(b) presents data for the Hall effect ρ_{xy} and ρ_{yx} for three gate voltages. Within the accuracy of the experiment the Hall effect is identical for the two directions of current flow. Close to $B=0$ the Hall effect is quenched and reveals a plateaulike structure around $B=0.2$ T. These latter phenomena have already been observed in square antidot lattices[5,12] and were explained by classical chaos and nonlinear resonances in the antidot lattice.[10] In square lattices the occurrence of the plateaulike structure in the Hall effect is related to the position of the maxima in the magnetoresistance.[5,10,12] This is clearly not the case in rectangular lattices as can be seen from Figs. 1(a) and 1(b).

In order to understand this remarkable situation in more detail let us first discuss the experimentally observed isotropic Hall effect via a gedanken experiment. Consider an electron gas that has a perimeter of square geometry and Ohmic contacts in the middle of each of the sides of the squares. The Hall effect would be measured by passing a current I_{ij} through contacts i and j that lie on opposing sides of the square. The Hall voltage V_{kl} then drops across the remaining two contacts k and l. According to Büttiker[13] such a four-terminal resistance $R_{ij,kl}=V_{kl}/I_{ij}$ obeys a generalized symmetry relation $R_{ij,kl}(B)=R_{kl,ij}(-B)$. In the case of the geometry considered above an exchange of current and voltage probes symbolizes two Hall measurements with current directions perpendicular to each other. Were the electron gas superimposed with a rectangular antidot lattice aligned along the sides of the square the additional symmetry results in $R_{ij,kl}(B)=-R_{ij,kl}(-B)$.[14] Although this argument for the Hall effect is strictly valid only in the case of a square geometry it should lead to similar results in the present experimental situation as long as the main axes of

the rectangular lattice are parallel to the current directions of the respective Hall geometries. This explains the observation as depicted in Fig. 1(b), that the Hall effect in a rectangular antidot lattice does not depend on the direction of current flow, i.e., $\rho_{xy} \cong \rho_{yx}$. It leads to the important conclusion that for a system with rectangular symmetry the features in the Hall effect can no longer be correlated with corresponding characteristics in the magnetoresistance in a straightforward manner.

The positions of the maxima in the magnetoresistance as presented in Fig. 1(a) can be evaluated in terms of a classical cyclotron diameter $2R_c = 2\sqrt{2\pi N_s \hbar/eB}$ where N_s is the carrier density as deduced from the high-field SdH oscillations. Figure 2 presents a survey of maxima positions in terms of cyclotron diameters for a range of carrier densities tuned via a gate voltage. For very small magnetic fields it it difficult to extract the precise position of the maxima in the magnetoresistance because of the underlying negative magnetoresistance. A distinct difference between the ρ_{xx} and ρ_{yy} data is that only ρ_{xx} exhibits maxima corresponding to cyclotron diameters $2R_c \leq 1$ μm. Maxima correspond to orbit diameters $2R_c$ close to $p_y = 0.5$ μm and $2p_y$. The size of these orbits is fairly constant as a function of carrier density. For smaller magnetic fields where the corresponding cyclotron orbits are larger than p_x or larger than many multiples of p_y, peaks occur in ρ_{xx} as well as in ρ_{yy}.

The general behavior and anisotropy of the magnetoresistance are very similar for all rectangular lattices studied. Figures 3(a) and 3(b) show a comparison of experimental results that were obtained on five samples with different ratios of $p_x:p_y$ and the same value of $N_s = 5\times10^{11}$ cm^{-2}. For all samples the short period is $p_y = 0.5$ μm and p_x is varied. Consequently $\rho_{xx}(B=0)$ is very similar for all samples because the resistance in this case is dominated by the region between two closely spaced antidots. For current flow along the short period of the lattice (ρ_{yy}) the $B=0$ resistance decreases for increasing p_x since the channels between the rows of antidots become wider. For the square lattice $p_x = p_y$ the magnetoresistance displays two pronounced maxima in $\rho_{xx} = \rho_{yy}$. According to Ref. 9 the higher-lying maximum is caused by electrons traveling around one antidot while the lower-lying peak corresponds to a deformed trajectory around four antidots. With increasing anisotropy of the rectangular lattice ρ_{xx} displays more maxima. On the other hand, ρ_{yy} shows less structure and finally reveals only one maximum for $p_x:p_y = 3:1$. These experimental results are discussed in the following on the basis of classical ballistic electron transport. For all samples investigated there is an overall negative magnetoresistance in ρ_{xx} as well as in ρ_{yy} for $0 < B < 1$ T. In previous work on square lattices this effect has been attributed to a

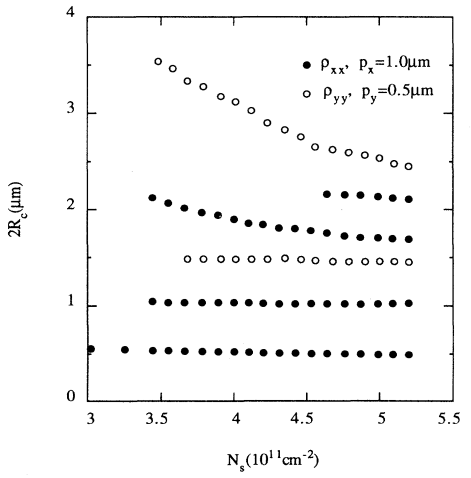

FIG. 2. Positions of the maxima in the magnetoresistance plotted in terms of a cyclotron diameter. The carrier density is tuned via a gate voltage. Positions are evaluated at absolute maxima of the resistance trace neglecting the underlying background.

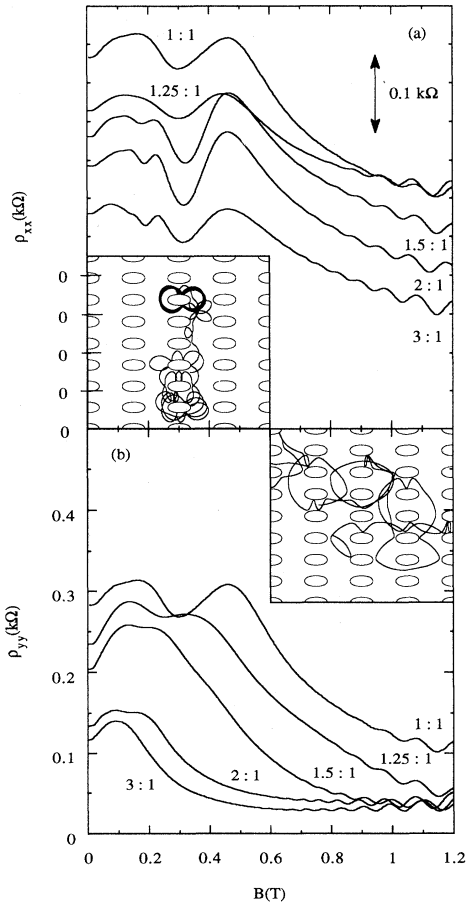

FIG. 3. (a) Magnetoresistance ρ_{xx} for current flow along the long period p_x of the lattice for a series of samples with different values of p_x. The carrier density is $N_s = 5\times10^{11}$ cm^{-2} and the short period is $p_y = 0.5$ μm for all samples. The curves are vertically offset for clarity. The inset shows a typical calculated electron trajectory for a magnetic field where the classical cyclotron diameter equals the short lattice period $2R_c = p_y$. The antidots are indicated by the contour lines where the potential energy is identical to the Fermi energy. (b) Magnetoresistance ρ_{yy} for current flow along the short period p_y of the lattice for the same series of samples as in (a). The inset presents a typical electron trajectory for a magnetic field where the classical cyclotron diameter equals $2R_c = 3.3p_y$.

magnetic-field-dependent localization process of the carriers.[3,5] In rectangular lattices there is a clear tendency [see Figs. 3(a) and 3(b)] that the ratio of high- to low-field magnetoresistance qualitatively reflects the anisotropy of the antidot lattice. In particular, for large anisotropies, the ρ_{yy} data are very similar to results obtained on quantum wires[15] in agreement with the comparable geometry of these two systems. However, a detailed explanation of the negative magnetoresistance in antidot lattices is missing so far and requires a thorough theoretical investigation.

It has been shown[9] that the conductivity σ of a square antidot lattice is given by the product $\sigma=\sigma^c(1-p_p)$, where p_p is the fraction of electrons that travel on pinned orbits around groups of antidots and σ^c is the conductivity of the carriers following chaotic trajectories. Naturally, also in a rectangular lattice pinned orbits will occur. In the linear response regime their existence should, however, not depend on the direction of current flow. We conclude that it is the conductivity σ^c of the carriers on chaotic trajectories that is responsible for the anisotropic transport. The highest-lying maximum in Fig. 3(a) is present for all five samples. This suggests that a pinned orbit around one antidot exists for all geometries. The corresponding maximum in ρ_{yy} [Fig. 3(b)] decreases in strength and finally vanishes for large anisotropies of the periodicities. In that case the electrons preferentially travel along a chaotic path in the wide channels between the rows of antidots and hardly encircle the pinned orbits around single antidots. The same is probably true for pinned orbits around two antidots that are much more likely to occur in a rectangular lattice as compared to a square lattice for geometrical reasons.

In order to calculate electron trajectories similarly as previously done for square lattices[4,7,9,10] we have solved the classical equations of motion in a potential landscape with rectangular symmetry. The insets in Figs. 3(a) and 3(b) present two typical trajectories for magnetic fields where the cyclotron diameter is equal to the shorter period $2R_c=p_y$ of the lattice (a) and $2R_c=3.3p_y$ (b). In the first case the electrons travel along a row of antidots and rarely cross from one row to the other. In the second case, where the cyclotron diameter covers several lattice periods, there is no spatial preference any more for the electron trajectory. In general, for magnetic fields, where the classical cyclotron diameter is smaller than the larger period of the lattice, we find that the carriers tend to travel along one row of antidots. They seldomly cross the region between the rows of antidots. If the cyclotron diameter is increased, the extent of typical electron trajectories becomes symmetric in both lateral dimensions. These results support the ideas that pinned electron orbits around small numbers of antidots preferentially affect ρ_{xx} where the current flow is along the long period of the lattice. The larger the diameter of a pinned orbit, i.e., the more antidots it encircles, the more it extends into the wide undamaged regions between the rows of antidots. Consequently, also the electrons that travel along the short period of the lattice should feel the existence of these pinned orbits resulting in a peak in ρ_{yy}. As in a square lattice[9] the pinned orbits are expected to be noncircular and it is therefore not a straightforward procedure to evaluate quantitatively the number of antidots that are encircled by pinned orbits corresponding to a given maximum in the magnetoresistance. The strong N_s dependence of the maxima positions corresponding to large orbits (see Fig. 2) also implies that these nonlinear effects are especially important for trajectories around large groups of antidots in agreement with theoretical considerations.[9] One pinned orbit may influence the conductivity in the two current directions differently. This could explain the different positions of the maxima in ρ_{xx} and ρ_{yy} for $2R_c>1$ μm.

In conclusion, magnetotransport experiments on rectangular antidot lattices are presented. It is found that the Hall effect does not depend on the direction of current flow with respect to the lattice orientation in agreement with symmetry arguments. This nontrivial result implies that features in the Hall effect and the magnetoresistance can no longer be correlated in a straightforward manner for rectangular lattices. The magnetoresistance is highly anisotropic and reveals maxima whose positions depend on the direction of current flow. It is argued that pinned electron orbits exist around groups of antidots similarly as in square lattices. In a rectangular lattice for current flow along the long period of the lattice preferentially pinned orbits around small groups of antidots are reflected in the magnetoresistance. For very low magnetic fields, where the classical cyclotron orbit covers several lattice periods in both lateral dimensions, pinned electron orbits influence the magnetoresistance similarly for both current directions.

We thank C. Lettau and A. Schmeller for the fertile collaboration with the ion irradiation system. We are grateful to M. Büttiker, D. Wharam, and W. Hansen for very valuable discussions and K. Häusler for initial support in the experiments. Financial support is gratefully acknowledged from the Deutsche Forschungsgemeinschaft and from the Esprit Basic Research Action.

[1]W. Hansen *et al.*, in *Semiconductors and Semimetals,* edited by M. Reed (Academic, San Diego, 1992), Vol. 35, p. 279.
[2]H. Fang *et al.*, Appl. Phys. Lett. **55**, 1433 (1989).
[3]K. Ensslin and P. M. Petroff, Phys. Rev. B **41**, 12 307 (1990).
[4]A. Lorke *et al.*, Phys. Rev. B **44**, 3447 (1991).
[5]D. Weiss *et al.*, Phys. Rev. Lett. **66**, 2790 (1991).
[6]K. Kern *et al.*, Phys. Rev. Lett. **66**, 1618 (1991).
[7]G. Berthold *et al.*, Phys. Rev. B **45**, 11 350 (1992).
[8]K. Ensslin *et al.*, Surf. Sci. **263**, 319 (1992).
[9]R. Fleischmann *et al.*, Phys. Rev. Lett. **68**, 1367 (1992).
[10]R. Ketzmerick, R. Fleischmann, and T. Geisel (unpublished).
[11]A. Scherer and M. L. Roukes, Appl. Phys. Lett. **55**, 377 (1989).
[12]R. Schuster *et al.*, Superlatt. Microstruct. **12**, 93 (1992).
[13]M. Büttiker, Phys. Rev. Lett. **57**, 1761 (1986). The symmetry relation as derived in this paper is much more general and even holds for an arbitrarily shaped and possibly disordered electron gas.
[14]This is not a trivial statement. If the main axes of the rectangular lattice were not oriented parallel to the sides of the square the Hall effect would not obey this symmetry relation.
[15]T. J. Thornton *et al.*, Phys. Rev. Lett. **63**, 2128 (1989).